Deuterium retention in tungsten exposed to low-energy and high-flux "clean[1]" and carbon-seeded deuterium plasmas

V.Kh. Alimov[1], J. Roth[2], R.A. Causey[3], D.A. Komarov[1], Ch. Linsmeier[2], A. Wiltner[2], F. Kost[2], S. Lindig[2]

[1]*Institute of Physical Chemistry and Electrochemistry, Russian Academy of Sciences, Leninsky prospect 31, 119991 Moscow, Russia*

[2]*Max-Planck-Institut für Plasmaphysik, EURATOM Association, Boltzmannstrasse 2, D-85748 Garching, Germany*

[3]*Sandia National Laboratories, P.O. Box 969, Livermore, CA 94550, USA*

1. Introduction

Tungsten and carbon fibre composites (CFC) are the candidate materials in the divertor region in ITER where the armors will be subjected to high flux (10^{22} m^{-2}s^{-1} or higher) deuterium-tritium plasmas [1]. Because of high sputtering yield and chemical erosion of the CFC materials, the sputtered carbon particles and hydrocarbon species can migrate into the plasma. They will be ionized by the energetic electrons and, together with hydrogen isotope ions, implanted into tungsten. Carbon and hydrocarbon impurities in the hydrogen plasma will not only govern the process of tungsten erosion and carbon deposition as reported in Ref. [2-8], but will create near-surface layers of tungsten carbides, W_2C and WC, depending on the conditions like the supply of thermal energy or particle bombardment [9-13], and also affect the surface deformation such as blistering [11, 14-16].

Despite of the fact that a great deal of publications was devoted to the hydrogen isotope retention in W materials [17-45], the influence of the carbon impurities in a hydrogen (deuterium, tritium) plasma or ion beam on the hydrogen isotope retention in W materials has not been examined yet. There are only indications that the vacuum conditions during D ion irradiation could influence deuterium retention in single crystal tungsten: a higher level of background impurities leads to a higher D retention [32, 43].

Studies of carbon re-deposition on polycrystalline tungsten in a controlled carbon-contaminated deuterium plasma environment were performed in the linear magnetized

---

[1] We use the term "clean" in quotation marks having in mind the impossibility to obtain absolutely clean plasma. In our case the conception "clean" D plasma means the plasma without intentionally introduced carbon impurities.

plasma facility PISCES-B [23]. Tungsten substrates were exposed to a high ion flux (10^{22} $m^{-2}s^{-1}$) and low energy ($\leq$100 eV/D) deuterium plasma for a total fluence of the order of 10^{26} D/m^2. Downstream CD_4 puffing was used to produce carbon impurities in the deuterium plasma at various substrate temperatures. At an impurity level of about 1% CD_4, no carbon deposition was observed on the plasma-exposed substrates at temperatures below 700 K. While the substrate temperature increased to 850 K, carbon particles started to form on the tungsten surface. Deuterium retention measurements were done using thermal desorption spectrometry. The dominant factors influencing the hydrogen isotope retention in plasma exposed tungsten were the substrate temperature, T_{exp}, and whether carbon was deposited on the tungsten surface. For uncontaminated tungsten surfaces the total isotope retention at $T_{exp} \leq$ 500 K was in the range from about 5×10^{20} to about 5×10^{21} D/m^2. These values were about one order of the magnitude higher than those after exposure at higher temperatures (>700 K). The deposited carbon increased the retention of deuterium which was mainly residing within the carbon film.

The retention of deuterium implanted at room temperature in pure and pre-irradiated with 40 keV C ions W single crystals was studied by Alimov et al. [46]. D ion implantation was performed at energies of 10 keV with the range confined in the carbon-modified layer and of 100 keV with the range exceeding the carbon-modified layer. The carbon pre-implantation influences the deuterium retention only if the range of the D ions is confined within the carbon-modified surface layer. In this case deuterium diffusion beyond the ion range does not occur and the retained amount of deuterium is smaller than in the pure W crystal. At a D ion energy where the deuterium range exceeds the carbon-modified layer the deuterium retention is the same for carbon-implanted and pure W samples.

For polycrystalline tungsten pre-irradiated with 1 keV C ions and subsequently implanted with 500 eV D ions, Poon et al. [47] observed that deuterium retention in carbon–implanted W strongly dependes on the C ion fluence and the implantation temperature. With a low C ion fluence, tungsten carbide WC was formed at the surface, leading to a decreased D retention at low D ion fluence, compared to the pure W case. With a high carbon ion fluence and low D ion fluence, the presence of a graphitic surface layer increases the D retention above the pure W case. With increasing D ion fluence, preferential sputtering removes both the graphitic surface layer and the implanted C from the bulk, such that the D retention behaviour of the specimen tends towards that of pure W (with no carbon ion pre-implantation) at high D ion fluences.

The purpose of this work consists in studying deuterium retention in monocrystalline and polycrystalline tungsten exposed to "clean" and carbon-seeded D plasmas at exposure

temperatures in the range from 313 to 853 K. Information about the total amount of deuterium retained in the W materials is obtained from thermal desorption measurements. Moreover, measurements of deuterium depth profiles can give detailed information about the fractions of deuterium retained both in the near-surface layers and in the bulk of the investigated materials. Therefore, the impact of carbon surface impurities on the D retention in the bulk of the plasma-exposed tungsten can be revealed. In our study the $D(^3He,p)^4He$ nuclear reaction at different ^3He energies was used for quantitative depth profiling.

2. Experimental

Two types of W materials were investigated:

(i) Single crystal tungsten specimens produced by double electron-beam zone melting. The manufacturer, the State Institute of Rare Metals (Moscow), quoted the purity as about 99.9 at.% with the main impurities being H (0.02 at.%), C (0.05 at.%) and O (0.05 at.%). The macro-crystallite sizes were in the range of 10-20 mm. The specimens were cut from a W rod by spark cutting and were 0.8-0.9 mm in thickness. The sample surface was parallel to the (100) crystallographic plane.

(ii) A hot-rolled polycrystalline tungsten foil (powder-metallurgy product, 99 at.% W, 0.03 at.% H, 0.1 at.% C, 0.2 at.% O, 0.1 at.% N, 0.5 at.% other impurities – Fe, Al, Si, Ni, Mg) has been investigated. The grain sizes were 1-5 μm. The samples were cut from the 0.5 mm thick foil by spark cutting.

The single-crystalline and polycrystalline W samples, 6×8 mm^2 in size, were mechanically and electrochemically polished.

The W samples were exposed to "clean" and carbon-seeded deuterium plasmas at various exposure temperatures T_{exp} in the range from 313 to 853 K at Institute of Physical Chemistry and Electrochemistry, Russian Academy of Sciences, Moscow (IPCE).

The "clean" plasma was generated in a planar dc magnetron operated with D_2 gas at a pressure of about 1 Pa. The samples placed on the cathode surface and covered with a tantalum mask with an aperture of 5 mm in diameter were bombarded with plasma ions accelerated in the cathode sheath of the magnetron discharge with a discharge voltage of 450 V. The spatial distribution of the plasma potential showed that the cathode-drop voltage was about 0.85 of the discharge voltage. Reasoning that D_2^+ ions dominate in the plasma, the mean energy of D ions was estimated to be about 200 eV. The ion flux was determined from ion current measurements and was 1.1×10^{21} D/(m^{2}s).

The carbon-seeded D plasmas were generated by placing plates of pyrolytic graphite within the sputter-dominated area of the cathode surface at distance of about 8 cm from the W sample. The plasma generated by using one graphite plate of about 7.5 cm^2 in surface area is denoted as "D+C(I)" plasma. The plasma generated by using two graphite plates with total surface area of about 15 cm^2 is denoted as "D+C(II)". Only polycrystalline W samples were exposed to the carbon-seeded D plasmas.

The W samples were exposed to the "clean" and carbon-seeded D plasmas for 30 min resulting in an ion fluence of 2×10^{24} D/m^2. During plasma exposure the sample temperature was measured by a chromel-alumel thermocouple welded to the front surface of the sample outside the irradiation area.

The deuterium profiles were determined by nuclear reaction analysis (NRA) at Max-Planck-Institut für Plasmaphysik, Garching (IPP). The D concentration within the near-surface layer (at depths up to about 0.5 μm) was measured by means of the D(^{3}He,α)H reaction at a ^{3}He energy of 0.69 MeV, and the α particles were energy-analyzed with a small-angle surface barrier detector with a solid angle of 9.17 msr at the laboratory scattering angle of 102°. The α spectrum was transformed into a D depth profile using the program SIMRNA [48]. To determine the D concentration at larger depths, an analyzing beam of ^{3}He ions with energies varied from 0.69 to 4.0 MeV was used. The protons from the D(^{3}He,p)^{4}He nuclear reaction were counted using a wide-angle proton detector with a solid angle of 0.15 sr placed at a scattered angle of 135°. The D(^{3}He,p)^{4}He nuclear reaction has a broad maximum at around 0.63 MeV which can be used for resonant depth profiling. In order to determine the D concentration profile in deeper layers, the computer program SIMNRA was used for the deconvolution of the proton yields measured at different ^{3}He ion energies. A deuterium depth distribution was assumed taking into account the near-surface depth profile obtained from the α particle spectrum, and the proton yield as a function of incident ^{3}He energy was calculated. The form of the D depth profile was then varied using an iterative technique until the calculated curve matched the measured proton yields [49].

The impurity concentration and chemical state in the outermost atomic layers on the tungsten surface was determined at IPP by X-ray photoelectron spectroscopy (XPS) which probes core-level transitions giving information on the specific element including its chemical environment (Table 1). All photoelectron spectra were measured using a monochromatic Al K_α source (E_{K_α} = 1486.6 eV). For survey spectra a pass energy of 93.9 eV was used. To achieve the highest energy resolution, the hemispherical energy

analyzer was driven at 2.95 eV pass energy yielding an energy resolution of 0.3 eV. The binding energy was calibrated with the Au $4f_{7/2}$ peak at 84.0 eV and Cu 2p and Ag 3d peaks for linearity. Depth profiles were acquired by sputtering with a scanned 3 keV Ar ion beam. The sputtered area was about 2×2 mm^2, and ion beam current on the target was about 0.4 μA.

To determine the binding energies and different fractions of binding states in the high-resolution XPS spectra, curve-fitting procedures were carried out using the MultiPak software package [51]. For the non-linear least-squares optimization procedure, a Gaussian-Lorentzian line shape was used and a Shirley background was applied [52].

Table 1. Binding energies for C 1s in carbon films and tungsten carbides [50] (preliminary data were published in [9])

Substance	Binding energy for C 1s [eV]
Graphitic carbon	284.2
Disordered graphitic carbon	285.1
W_2C	283.4
WC	282.9

The surface morphology of the plasma-exposed W samples was investigated by scanning electron microscope (SEM).

3. Results

3.1. Deuterium depth profiles

The retention of deuterium in tungsten develops differently at different depths. The depth at which deuterium is retained in the W materials irradiated with low-energy D ions or exposed to a D plasma is divided into three zones: (i) the near-surface layer (up to a depth of 0.2-0.5 μm, depending on the ion energy), (ii) a sub-surface layer (from about 0.5 to about 3 μm), and (iii) the bulk (> 6 μm) [39].

In the single-crystalline and polycrystalline W materials exposed to the "clean" low-energy (≈200 eV/D) and high-flux (about $1×10^{21}$ D/m^{2}s) magnetron D plasma at exposure

temperatures of T_{exp} = 303-313 K, the D depth profiles are characterized by a sharp near-surface concentration maximum of about 1 at.% and a decreasing concentration tail into the bulk (Fig. 1). At T_{exp} = 413-493 K, the D profiles demonstrate, in addition to the near-surface peak, a relatively high D concentration (0.3-0.4 at.%) in the sub-surface layer. The main difference between single-crystalline and polycrystalline W materials is the constant concentration level in the bulk for polycrystalline material which is absent in single crystals.

The concentration of D_2 molecules (in arbitrary units) within the near-surface layer of the W crystal was determined by measuring D_2 release rate in the course of surface sputtering with Ar ions (residual gas analysis, RGA, by quadrupole mass spectrometer). A characteristic of the D_2 release rate after exposure to the "clean" D plasma at T_{exp} = 373 K is that repetitive D_2 gas bursts occur throughout the whole analysis time corresponding to a depth of ~450 nm (Fig. 2). The appearance of D_2 molecules is related to the formation of voids filled by gaseous deuterium. Based on the D depth profiles (Fig. 1), one may assume the void formation at depths at least up to 1-2 μm.

In the W single crystal exposed to the "clean" D plasma, the deuterium retention is about 1×10^{20} D/m^2 at T_{exp} = 303 K and, as exposure temperature further increases, rises to its maximum of about 4×10^{20} D/m^2 at T_{exp} = 463 K and then decreases down to about 2×10^{19} D/m^2 at T_{exp} = 533 K (Fig. 3 a). In the polycrystalline W exposed to the "clean" D plasma, the D retention demonstrates practically the same temperature dependence as that in the W single crystal, but the maximum retention in the polycrystalline W is about 5×10^{20} D/m^2 at T_{exp} = 493 K (Fig. 3 a). Both in single-crystalline and polycrystalline W exposed to the "clean" D plasma at T_{exp} = 303-313 K, the retention in the near-surface (at depths from 0 to 0.3 μm) is higher than that in the sub-surface layer and in the bulk (at depths from 0.3 to 7 μm), whereas at T_{exp} above 350 K the D retention at depths above 0.3 μm starts to be dominating and reaches about 90% of the total D retention at T_{exp} = 450-500 K (Fig. 4).

In the polycrystalline W irradiated with 200 eV D ions at low flux (about 4×10^{19} D/m^{2}s), the D retention decreases drastically as the irradiation temperature increases from 323 to 393 K (Fig. 3 a). The D retention with a maximum at higher temperature is observed when the W materials are exposed to high flux D plasma. Data on the D retention in polycrystalline W exposed to low-energy (about 100 eV/D) and high flux (about 1×10^{22} m^{-2}s^{-1}) hydrogen isotope plasmas taken from Refs. [21, 27, 42, 45] are shown in Fig. 3 b. As seen from the figure, for the ion fluxes of about 1×10^{22} m^{-2}s^{-1} a drastic decrease in the D retention is observed at the exposure temperatures above 650-700 K. In our experiments

with the ion flux of about 1×10^{21} m^{-2}s^{-1}, the decrease in the D retention begins at about 500 K. Evidently, the ion flux affects not only the D retention in W materials, as it was reported in [27, 32], but also the temperature where the D retention reaches its maximum.

The D depth profiles in the polycrystalline W exposed to the carbon-seeded D plasmas ("D+C(I)" and "D+C(II)" plasmas) (Fig. 5) at first sight are similar to those measured after "clean" D plasma exposure (Fig. 1). However, after exposure to carbon seeded plasmas the near-surface concentration maximum is about 3 at.% (compare with about 1 at.% for the "clean" D plasma exposure), and the exposure temperature when the D profiles demonstrate a maximum D concentration at depths of 2-3 μm is higher than that for the "clean" D plasma exposure. It is significant that in the W samples exposed to the carbon-seeded D plasmas at temperatures above 600 K, the D concentration in the bulk (at depths beyond 6 μm) is about one order of magnitude higher than that after exposure to the "clean" D plasma (compare Figs. 1 and 5).

After exposure to carbon-seeded D plasmas, the maximum D retention is observed at the exposure temperatures of 603 K ("D+C(I)" plasma) and 563 K ("D+C(II)" plasma), whereas for "clean" D plasma exposure the maximum retention is at T_{exp} = 493 K (Fig. 4). Generally, maximum D retention after exposure to carbon seeded plasmas at elevated temperatures is $(5-9) \times 10^{20}$ D/m^2 and is comparable to the maximum retention after exposure to a "clean" D plasma.

The temperature dependences of the D content in the near-surface layer (at depths from 0 to 0.3 μm) for exposure to the "clean" and carbon-seeded D plasmas are different (Fig. 4 a). If for the "clean" D plasma exposure the D content is about 5×10^{19} D/m^2 at T_{exp} = 313 K and starts to fall drastically at the exposure temperature of about 500 K, that for the carbon-seeded D plasma exposure the D content in the near-surface layer is 1×10^{20} D/m^2 at low exposure temperatures and starts to decrease slowly at the exposure temperature of about 600 K. As evident from XPS spectra (see paragraph 3.3), for the carbon-seeded plasmas the degree of covering of the W surface with an amorphous deuterated carbon film is higher then that for the "clean" D plasma.

As for the "clean" D plasma exposure, the D content at depths from 0.3 to 7 μm in polycrystalline exposed to carbon-seeded D plasmas T_{exp} = 400-700 K is higher that that in the near-surface W layer (Fig. 4 b).

3.2. Formation of blisters

SEM micrographs of the single-crystalline W exposed to the "clean" D plasma and micrographs of the polycrystalline W exposed to the "clean" and carbon-seeded D plasmas to an ion fluence of 2×10^{24} D/m^2 at various exposure temperatures are shown in Figs. 6-8. Dome-shaped elevations named blisters are formed on the metal surface exposed to the D plasmas at elevated temperatures. The shapes of most blisters are almost spherical with sizes ranging from about 2 to 50 μm, depending on the W structure and conditions of the D plasma exposure.

After exposure to the "clean" D plasma at T_{exp} = 303 K, the blisters are not formed on the surface of the single-crystalline W sample. However, after exposure at temperatures in the range from 373 to 533 K blisters appear on the surface of the W crystals, and the size (diameter) of blisters is 1-5 μm (Fig. 6). The maximum areal density of blisters is observed at T_{exp} = 413-463 K, whereas at T_{exp} = 533 K only solitary blisters are present on the surface (Fig. 6 b).

For the polycrystalline W exposed both to the "clean" D plasma at T_{exp} = 418-493 K and to the carbon-seeded D plasma at T_{exp} = 463-603 K, cracks are observed on the surface of blister lids (Fig. 7 b). Note that after exposure to the D plasmas at these temperatures the D depth profiles demonstrate the concentration minimum between the near-surface and bulk maxima (Figs. 1 b and 5). The maximum areal density of blisters is observed at T_{exp} = 493 K for the "clean" D plasma and at T_{exp} = 533-603 K for the carbon-seeded D plasmas. At these exposure temperatures the D content at depths beyond 0.3 μm reaches its maximum (Fig. 4 b).

The dependence of blister mean size (diameter) on the exposure temperature for the polycrystalline W is shown in Fig. 9. For the "clean" D plasma exposure, the mean blister size is about 3 μm at T_{exp} = 313 K and grows to the maximum value of about 30 μm at T_{exp} = 573 K (Fig. 8 a). At a higher exposure temperature the blister size starts to decrease. For the carbon-seeded D plasma exposure, the blister size demonstrates the opposite temperature dependence. At T_{exp} = 363-413 K the mean blister size is around 50 μm and decreases to about 20 μm at the exposure temperature of 563 K (Fig. 8 b). Further increase of the exposure temperature leads to the growth of the blisters in size. It should be noted that a tungsten carbide layer is formed on the W surface during exposure to the carbon-seeded D plasmas and is not formed during exposure to the "clean" D plasma.

For exposure to both the "clean" and carbon-seeded D plasmas at T_{exp} above 680 K, no blister formation is observed on all W surfaces (Fig. 9).

3.3. Surface composition

The carbon, oxygen, and tungsten concentration on the surface of the polycrystalline W exposed to the "clean" and carbon-seeded D plasmas was determined from the survey XPS spectra (an example is shown in Fig. 10). The elemental concentrations are calculated from the survey spectra using tabulated sensitivity factors Since no elemental depth profile within the XPS information depth (several nm) is available, the concentrations are calculated assuming a homogeneous distribution over this range. In the survey spectra the signals from Na, N and Cu are detected in addition to the expected peaks of C, O and W. Cu is presumably sputtered from copper parts in the magnetron device and co-deposited during exposure to the D plasmas. After the plasma exposure the samples were kept in air until the XPS analysis was carried out and Na, N, and C impurity accumulation at the top surface could be attributed to the air exposure. The high C concentrations (around 50 at.%) measured directly after sample loading (before Ar sputtering) are typically observed on samples which were carried through the air. These adsorbed layers can be easily removed by sputtering with low Ar fluences. Therefore, we took into consideration the results obtained after surface sputtering with fluences above 1×10^{19} Ar/m^2. In all cases, the remaining concentrations of the detected impurities (besides carbon and oxygen) are below 1 at.% and are not expected to influence the deuterium inventory.

Although all samples contain carbon in the surface layer, the concentration is lowest for the samples exposed to the "clean" D plasma. The carbon concentration in the near-surface layers in these cases does not exceed 18 at.% (Table 2). After exposure to the carbon-seeded plasmas, however, the C concentration always exceeds 25 at.%.

The chemical state of the carbon presented at the surface is determined in high-resolution C 1s spectra. Disordered graphitic carbon (peak at binding energy of 285.1 eV) is found on the W samples exposed both to the "clean" and carbon-seeded D plasmas. Contaminations from the air usually also show peaks at higher binding energies in the C 1s region (around 289 eV) and are not any more present after the lowest applied sputtering fluence of 1×10^{19} Ar/m^2, therefore we concluded that contaminations from the transport through the air have largely been removed by gentle Ar sputtering procedure.

For the polycrystalline W exposed to the "clean" D plasma, no indications for carbide formation are visible in the C 1s core-level XPS spectra measured after sputtering with Ar ions at fluences below 7.5×10^{19} Ar/m^2 (Fig. 11). Since Ar ion bombardment also leads to the formation of carbides already at 300 K [53], the absence of carbide intensity in these spectra indicates that no tungsten carbides are present in the surface after the

exposure to the "clean" D plasma. In the spectra measured after the surface sputtering with fluences above 7.5×10^{19} Ar/m^2, small peaks at the carbide positions are detected (not shown here) and can be explained by the influence of the Ar ion beam.

For the polycrystalline W exposed to the carbon-seeded plasmas, however, the C 1s core-level XPS spectra measured after surface sputtering with lowest Ar ion fluence (1×10^{19} Ar/m^2) indicate clearly peaks for tungsten subcarbide W$_2$C (at binding energy of 283.4 eV) (Fig. 11). The appearance of this peak can be explained by the implantation of carbon from the carbon-seeded plasmas into the tungsten surface and the formation of carbide by the energetic C atoms. Assuming formation of tungsten carbide with a stoichiometry of W$_2$C and analyzing data on the impurity concentration in the near-surface layer of polycrystalline W exposed to the "pure" and carbon-seeded D plasmas (Table 2), the coverage of W surface with carbide phase can be estimated to be 20-40% for the D+C(I) plasma and 55-60% for the D+C(II) plasma.

Table 2. The impurity concentration in the near-surface layer of polycrystalline W exposed to the "pure" and carbon-seeded D plasmas. The XPS measurements were carried out after surface sputtering with 3 keV Ar ions at a fluence of 1×10^{19} Ar/m^2.

Type of plasma // exposure temperature	W [at.%]	O [at.%]	C (total) [at.%]	C (in carbide phase) [at.%]	C (in carbide phase) to W atomic ratio
"clean" D plasma // T_{exp} = 418 K	52.0	35.9	12.1	1.6	0.03
"clean" D plasma // T_{exp} = 463 K	34.5	47.6	17.9	0	0
"D+C(I)" plasma // T_{exp} = 413 K	41.8	32.6	25.6	8.0	0.19
"D+C(I)" plasma // T_{exp} = 603 K	46.9	24.4	28.7	5.0	0.11
"D+C(II)" plasma // T_{exp} = 383 K	30.4	25.3	44.3	8.9	0.29
"D+C(II)" plasma // T_{exp} = 563 K	37.2	35.2	27.6	10.2	0.27

Oxygen atoms are present on the W surfaces both after "clean" and carbon-contaminated D plasma exposures. The oxygen concentration shows no dependency on the type of the plasma.

4. Discussion

The high deuterium concentration in the sub-surface layer and the formation of blisters allows the conclusion that exposure to a low-energy and high ion flux D plasma modifies the surface to depths of up to 2-4 μm, both for W single crystals and polycrystalline W. The sputter-RGA measurements show that a part of deuterium is accumulated in the form of D_2 molecules in the near-surface layer (Fig. 2). It could be supposed that D_2 molecules (or rather D_2-filled voids) are formed in the sub-surface layer also (up to depths of several micrometers). According to van Veen et al. [54], the D_2 gas inside the voids is expected to be released during annealing at 400-600 K (detrapping energy ~1.0 eV), whereas the D atoms bound on the inner surface of voids (binding energy ~1.7 eV) is expected to be released at 700-900 K. Actually, the D depth profiles (Figs. 1 and 5) show that the D concentration at depths of 1-3 μm starts to decrease significantly at the exposure temperatures above 500 K confirming the assumption about formation of the D_2-filled voids.

The depths of D accumulation (several micrometers) are much larger than the deuterium implantation range (several nanometers). Moreover, deuterium ions with energies less than 800 eV are not able to produce displacement damage in tungsten [22]. A review of hydrogen bubbles in metals by Condon and Schober [55] outlines a possible mechanism of void formation - the mechanism of near-surface plastic deformation caused by the deuterium supersaturation within the near-surface layer. During D ion irradiation or D plasma exposure the D concentration in the implantation zone greatly exceeds the solubility limit and stresses the matrix lattice until plastic deformation with formation of voids and vacancy clusters occurs to alleviate these tensions. This deformation is assumed to be responsible for the sudden increase in trapping sites for deuterium and the concurrent accumulation of deuterium, both in the form of D_2 molecules and D atoms. Traces of the plastic deformation within the sub-surface layer of the W single crystal are observed on the surface as etching pits (Luder's bunds) oriented along certain crystallographic plane (Fig. 7 a). These etching pits are created due to preferential sputtering of dislocation lines intersecting the surface. According to Savitsky and Burkhanov [56], at plastic deformations of 6-10% the dislocation lines in the bcc lattice are parallel to the direction of the closest packing. But at higher degree of the deformation, a texture is formed.

It has been shown recently [39] that after irradiation with 200 eV D ions at a low flux of about 4×10^{19} D/m^{2}s, the maximum concentration of deuterium (rather D$_2$ molecules) at depths of 1-3 μm in the polycrystalline W specimen is at least one order of magnitude higher than that in the W single crystals. This suggests that the initial structure of the W materials plays a major role in the stress-induced void formation. Possibly, the grain boundaries serve as preferential sites for void nucleation and growth. However, after exposure to the high-flux (1.1×10^{21} D/m^{2}s) D plasma, the maximum D concentration in the sub-surface layer (at depths of 1-3 μm) is 0.3-0.4 at.% both in the W single crystal and polycrystalline W (Fig. 1). Apparently, for high-flux D ion implantation formation of the stress-induced defect depends on the W structure to a lesser degree than for low-flux implantation.

In the polycrystalline W exposed to the carbon-seeded D plasma, the temperature of maximum retention of deuterium (rather in the form of D$_2$ molecules) is shifted by 100 K towards higher temperatures as compared to the "clean" D plasma exposure. Additionally, for the carbon-seeded D plasma exposure the D concentration at intrinsic defects (beyond 6 μm) at the exposure temperatures above 600 K is about one order of magnitude higher than that for the "clean" D plasma exposure. We expect that the tungsten carbide layer on tungsten surfaces formed by simultaneous deuterium and carbon implantation could prevent the implanted deuterium from leaving the tungsten [15]. As a result, the flux of deuterium atoms diffusing into the bulk increases. In doing so, the temperature of the maximum deuterium retention in the zone of the stress-induced defects is shifted from about 500 to about 600 K (Fig. 4 b), and the concentration of deuterium trapped at intrinsic defects at higher exposure temperatures significantly increases.

According to van Veen et al. [54], the maximum temperature at which molecular deuterium can be accumulated in voids is about 600 K, therefore one might expect that at higher fluxes of deuterium atoms diffusing into the bulk the maximum retention at depths of 1-3 μm will be observed at about 600 K. At that, the concentration of D atoms trapped at intrinsic defects in the bulk might be increased.

Ueda et al. [15] proposed two mechanisms to control deuterium migration through a tungsten carbide layer. One is to decrease deuterium diffusion through the tungsten carbide layer, and other is to reduce the recombination rate of deuterium atoms on the surface. Regarding the hydrogen diffusion in tungsten carbide, Atsumi et al. [57] have reported data indicating that the diffusivity of hydrogen isotopes in tungsten carbide layer is very different from that in pure W. In these experiments hydrogen absorption was measured

under a hydrogen atmosphere of about 10 kPa. They showed that coexisting carbon with tungsten strongly suppressed hydrogen retention and diffusion in tungsten. Deuterium depth profiles in chemical vapor deposited tungsten carbides W_2C and WC [58] and in the polycrystalline W exposed to the low-energy and high ion flux D plasma to the same ion fluence at temperatures below 500 K show that D atoms penetrate in the polycrystalline W much deeper than in tungsten carbides. Thus, these results suggest that tungsten carbide layers formed on the W surface during exposure to the carbon-seeded D plasmas act as a diffusion barrier to deuterium.

Concerning the recombination of hydrogen atoms on the surface, there is no reliable data so far. According to Ogorodnikova [36] and Ueda et al. [15], the presence of carbon atoms on the W surface, however, can reduce the recombination rate of hydrogen atoms.

Both the carbide barrier layer for D diffusion and the reduced recombination rates lead to the build-up of high D concentrations in the nearest-surface layer, to a larger in-depth migration of deuterium, and finally to a larger probability of vacancy cluster and void formation in deeper layers. In doing so, formation of deuterium-defects complexes/voids may occur at higher exposure temperature (at about 600 K) than that in the case of the W surface without the tungsten carbide layer (at about 500 K).

Recent observation of modification of tungsten surfaces exposed to low energy and high flux plasmas and ion beam bombardment have shown the formation of blisters [22, 23, 27, 37, 42, 45, 59-61]. In our experiments at the exposure temperatures between 350 and 500 K, in spite of the same D retention, the mean size of blisters after the carbon-seeded D plasma exposure is by about one order of magnitude larger than that after the "clean" D plasma exposure. Mechanical properties of tungsten carbides (the Poisson's ratio, the shear modulus) are thought to differ from those for pure W. Possibly, these parameters are the reason for the different sizes of the blisters formed at the same temperature under exposure to the "clean" and carbon-seeded D plasmas.

There are mainly two different models which describe the blistering process. One is the gas driven model [62-64], in which bubbles are assumed to grow by coalescence or the loop punching mechanism [65]. As more deuterium is deposited and bubbles grow, cooperative fracture between the bubbles suddenly becomes an easy way of relieving their overpressure, thus initiating cracks, allowing internal gas release, and lifting the surface off the implanted material into dome-shaped blisters. Another is the lateral stress model [66, 67] in which stresses are assumed to be introduced in the implanted layer and the surface will buckle if the induced stress becomes too high.

After exposure to the "clean" D plasma at $T_{exp} = 573$ K to an ion fluence of 2×10^{24} D/m^2, the blister size (diameter) reaches 30 μm (Fig. 9), while the concentration of deuterium is relatively low (about 10^{-2} at.%). This fact points to the lateral stress model to describe the blister formation mechanism.

5. Conclusions

Depth profiles of deuterium trapped in single-crystalline and polycrystalline W exposed to a low energy ($\approx$200 eV/D) and high deuterium ion flux (1.1×10^{21} D/m^{2}s) in "clean" and carbon-seeded D plasmas at a fluence of about 2×10^{24} D/m^2 and temperatures from 313 to 853 K have been measured using the D(^{3}He,p)^{4}He nuclear reaction, analyzing both the α particles and protons. To determine the D concentration at depths up to 7 μm, an analyzing beam of ^{3}He ions with energies from 0.69 to 4.0 MeV was used.

In the case of the "clean" D plasma exposure, the total deuterium retention in single-crystalline and polycrystalline W increases with the exposure temperature, reaching its maximum value of 5×10^{20} D/m^2 at about 500 K, and then decreases as the temperature grows further. Seeding of carbon into the D plasma does not significantly change the maximum D retention in the polycrystalline W, but shifts the temperature at which the D retention peaks are at maximum, to about 600 K. The high D concentration (about 0.3 at.%) at depths of 1-3 μm, observed after exposure to the "clean" and carbon-seeded D plasma at temperatures of the maximum D retention, is due to accumulation of D$_2$ molecules in voids created during D plasma exposure. At exposure temperatures above 600 K deuterium is retained in the polycrystalline W as D atoms chemisorbed at the walls of microvoids initially presented in the hot-rolled powder-metallurgy W matrix.

It can be assumed that tungsten carbide is formed on the W surface under exposure to the carbon-seeded D plasmas, it serves as a barrier layer for diffusion and prevents the outward transport of deuterium, thus increasing the D retention in the bulk of polycrystalline W matrix.

D plasma exposure with ion energies well below the displacement threshold modifies the W structure to depths of up to about 5 μm, both in W single crystals and polycrystalline W. Plastic deformation of the W surface caused by deuterium super-saturation within the near-surface layer is suggested as a mechanism for D$_2$-filled void formation.

References

[1] G. Federici, P. Andrew, P. Barabaschi, J. Brooks, R. Doerner, A. Geier, A. Herrmann, G. Janeschitz, K. Krieger, A. Kukushkin, A. Loarte, R. Neu, G. Saibene, M. Shimada, G. Strohmayer, and M. Sugihara, J. Nucl. Mater. 313-316 (2003) 11.

[2] D. Naujoks, W. Eckstein, J. Nucl. Mater. 220-222 (1995) 993.

[3] D. Naujoks, W. Eckstein, J. Nucl. Mater. 230 (1996) 93.

[3] D. Hildebrandt, P. Wienhold, W. Schneider, J. Nucl. Mater. 290-293 (2001) 89.

[4] R. Kawakami, K. Ohya, J. Nucl. Mater. 313-316 (2003) 107.

[5] R. Kawakami, T. Shimada, Y. Ueda, M. Mishikawa, J. Nucl. Mater. 329-333 (2004) 737.

[6] T. Mitani, R. Kawakami, S. Kuriu, J. Nucl. Mater. 329-333 (2004) 830.

[7] R. Kawakami, T. Mitani, J. Nucl. Mater. 337-339 (2005) 45.

[8] R. Kawakami, J. Nucl. Mater. 348 (2006) 256.

[9] J. Luthin, Ch. Linsmeier, Surf. Sci. 454–456 (2000) 78.

[10] J. Luthin, Ch. Linsmeier, J. Nucl. Mater. 290-293 (2001) 121.

[11] T. Shimada, Y. Ueda, M. Nishikawa, Fusion Eng. Design 66-68 (2003) 247.

[12] T. Shimada, T. Funabiki, R. Kawakami, Y. Ueda, M. Nishikawa, J. Nucl. Mater. 329-333 (2004) 747.

[13] Y.Ueda, M. Fukumoto, I. Sawamura, D. Sakizono, T. Shimada, M. Nishikawa, Fusion Eng. Design 81 (2006) 233.

[14] Y. Ueda, H. Kikuchi, T. Shimada, A. Sagara, B. Kyoh, M. Nishikawa, Fusion Eng. Design 61&62 (2002) 255.

[15] Y. Ueda, T. Shimada, M. Nishikawa, Nucl. Fusion 44 (2004) 62.

[16] T. Shimada, H. Kikuchi, Y. Ueda, A. Sagara, M. Nishikawa, J. Nucl. Mater. 313-316 (2003) 204.

[17] R.A. Anderl, D.F. Holland, G.R. Longhurst, R.J. Pawelko, C.L. Trybus, C.H. Sellers, Fusion Technol. 21 (1992) 745.

[18] R. Sakamoto, T. Muroga, N. Yoshida, J. Nucl. Mater. 220-222 (1995) 819.

[19] V.Kh. Alimov, B.M.U. Scherzer, J. Nucl. Mater. 240 (1996) 75.

[20] A.A. Haasz, J.W. Davis, M. Poon, R.G. Macaulay-Newcombe, J. Nucl. Mater. 258-263 (1998) 889.

[21] R. Causey, K. Wilson, T. Venhaus, W.R. Wampler, J. Nucl. Mater. 266-269 (1999) 467.

[22] A.A. Haasz, M. Poon, J.W. Davis, J. Nucl. Mater. 266-269 (1999) 520.

[23] F.C. Sze, L. Chousal, R.P. Doerner, S. Luckhardt, J. Nucl. Mater. 266-269 (1999) 1212.

[24] S. Nagata, K. Takahiro, S. Horiike, S. Yamaguchi, J. Nucl. Mater. 266-269 (1999) 1151.

[25] S. Nagata, K. Takahiro, J. Nucl. Mater. 283-287 (2000) 1038.

[26] A.A. Haasz, M. Poon, R.G. Macaulay-Newcombe, J.W. Davis, J. Nucl. Mater. 290-293 (2001) 85.

[27] T. Venhaus, R. Causey, R. Doerner, T. Abeln, J. Nucl. Mater. 290-293 (2001) 505.

[28] V.Kh. Alimov, K. Ertl, J. Roth, J. Nucl. Mater. 290-293 (2001) 389.

[29] V.Kh. Alimov, K. Ertl, J. Roth, K. Schmid, Physica Scripta T94 (2001) 34.

[30] V.Kh. Alimov, A.P. Zakharov, R.Kh. Zalavutdinov, in: A. Hassanein (Ed.), Hydrogen and Helium Recycling at Plasma Facing Materials, NATO Science Series II, vol. 54, Kluwer Academic, 2002, p. 131.

[31] R.G. Macaulay-Newcombe, A.A Haasz, M. Poon, J.W. Davis, in: A. Hassanein (Ed.), Hydrogen and Helium Recycling at Plasma Facing Materials, NATO Science Series II, vol. 54, Kluwer Academic, 2002, p. 145.

[32] M. Poon, R.G. Macaulay-Newcombe, J.W. Davis, A.A. Haasz, J. Nucl. Mater. 307-311 (2002) 723.

[33] B.M. Oliver, T.J. Venhaus, R.A. Causey, F.A. Garner, S.A. Maloy, J. Nucl. Mater. 307-311 (2002) 1418.

[34] H. Iwakiri, K. Morishita, N. Yoshida, J. Nucl. Mater. 307-311 (2002) 135.

[35] M. Poon, A.A. Haasz, J.W. Davis, R.G. Macaulay-Newcombe, J. Nucl. Mater. 313-316 (2003) 199.

[36] O.V. Ogorodnikova, J. Roth, M. Mayer, J. Nucl. Mater. 313-316 (2003) 469.

[37] W. Wang, J. Roth, S. Lindig, C.H. Wu, J. Nucl. Mater. 299 (2001) 124.

[38] V.Kh. Alimov, Physica Scripta T 108 (2004) 46.

[39] V.Kh. Alimov, J. Roth, M. Mayer, J. Nucl. Mater. 337-339 (2005) 619.

[40] B.M. Oliver, R.A. Causey, S.A. Maloy, J. Nucl. Mater. 329-333 (2005) 977.

[41] D. Nishijima, T. Sugimoto, H. Iwakiri, M.Y. Ye, N. Ohno, N. Yoshida, S. Takamura, J. Nucl. Mater. 337-339 (2005) 927.

[42] K. Tokunaga, M.J. Baldwin, R.P. Doerner, N. Noda, Y. Kubota, N. Yoshida, T. Sogabe, T. Kato, B. Schedler, J. Nucl. Mater. 337-339 (2005) 887.

[43] M. Poon, R.G. Macaulay-Newcombe, J.W. Davis, A.A. Haasz, J. Nucl. Mater. 337-339 (2005) 629.

[44] K. Katayama, T. Kawasaki, Y. Manabe, H. Nagase, T. Takeishi, M. Nishikawa, Thin Solid Films 506-507 (2006) 188.

[45] G.-N. Luo, W.M. Shu, M. Nishi, Fusion Eng. Design 81 (2006) 957.

[46] V.Kh. Alimov, K. Ertl, J. Roth, K. Schmid, J. Nucl. Mater. 282 (2000) 125.

[47] M. Poon, J.W. Davis, A.A. Haasz, J. Nucl. Mater. 283-287 (2000) 1062.

[48] M. Mayer, SIMNRA User's Guide, Tech. Rep. IPP 9/113, Garching, 1997, and www.rzg.mpg.de/~mam.

[49] V.Kh. Alimov, M. Mayer, J. Roth, Nucl. Instr. and Meth. B 234 (2005) 169.

[50] J. Luthin, Chemical Interaction During the Formation Carbon-Based Mixed Materials, Ph.D. Thesis, Max-Planck-Institut für Plasmaphysik, IPP Report 9/129, 2001 (in German).

[51] MultiPak, Ver. 7.0.1, Physical Electronics (2004).

[52] D.A. Shirley, Phys. Rev. B 5 (1972) 4709.

[53] J. Luthin, H. Plank, J. Roth, Ch. Linsmeier, Nucl. Instr. and Meth. B 182 (2001) 218.

[54] A. van Veen, J. de Vries, D. Segers, and G.J. Rozing, in: P.C. Jain, R.M. Singru and K.P. Gopinathan (Eds.), Positron Annihilation, World Scientific Publ. Co., Singapore, 1985, p. 543.

[55] J.B. Condon and T. Schober, J. Nucl. Mater. 207 (1993) 1.

[56] E.M. Savitsky, G.S.Burkhanov, Single Crystals of Refractory and Less-Common Metals and Alloys, Nauka, Moscow, 1972 (in Russian).

[57] H. Atsumi, T. Tanabe, J. Nucl. Mater. 258-263 (1998) 896.

[58] V.Kh. Alimov and J. Roth, Private communication (2007).

[59] F.C. Sze, R.P. Doerner, S. Luckhardt, J. Nucl. Nater. 264 (1999) 89.

[60] M.Y. Ye, H. Kanehara, S. Fukuda, N. Ohno, S. Takamura, J. Nucl. Nater. 313-316 (2003) 72.

[61] G.-N. Luo, W.M. Shu, M. Nishi, J. Nucl. Mater. 347 (2005) 111-117.

[62] J.H. Evans, J. Nucl. Mater. 76&77 (1978) 228.

[63] S.K. Das, M. Kaminsky, G. Fenske, J. Nucl. Mater. 76&77 (1978) 215.

[64] S.K. Das, M. Kaminsky, G. Fenske, J. Appl. Phys. 50 (1979) 3304.

[65] G.W. Greenwood, A.J.E. Foreman, D.E. Rimmer, J. Nucl. Mater. 4 (1959) 305.

[66] J. Roth, in: Applications of Ion Beams to Materials, eds. G. Carter, J.S. Colligan, N.A. Grant (The Institute of Physics, London 1976) p. 280.

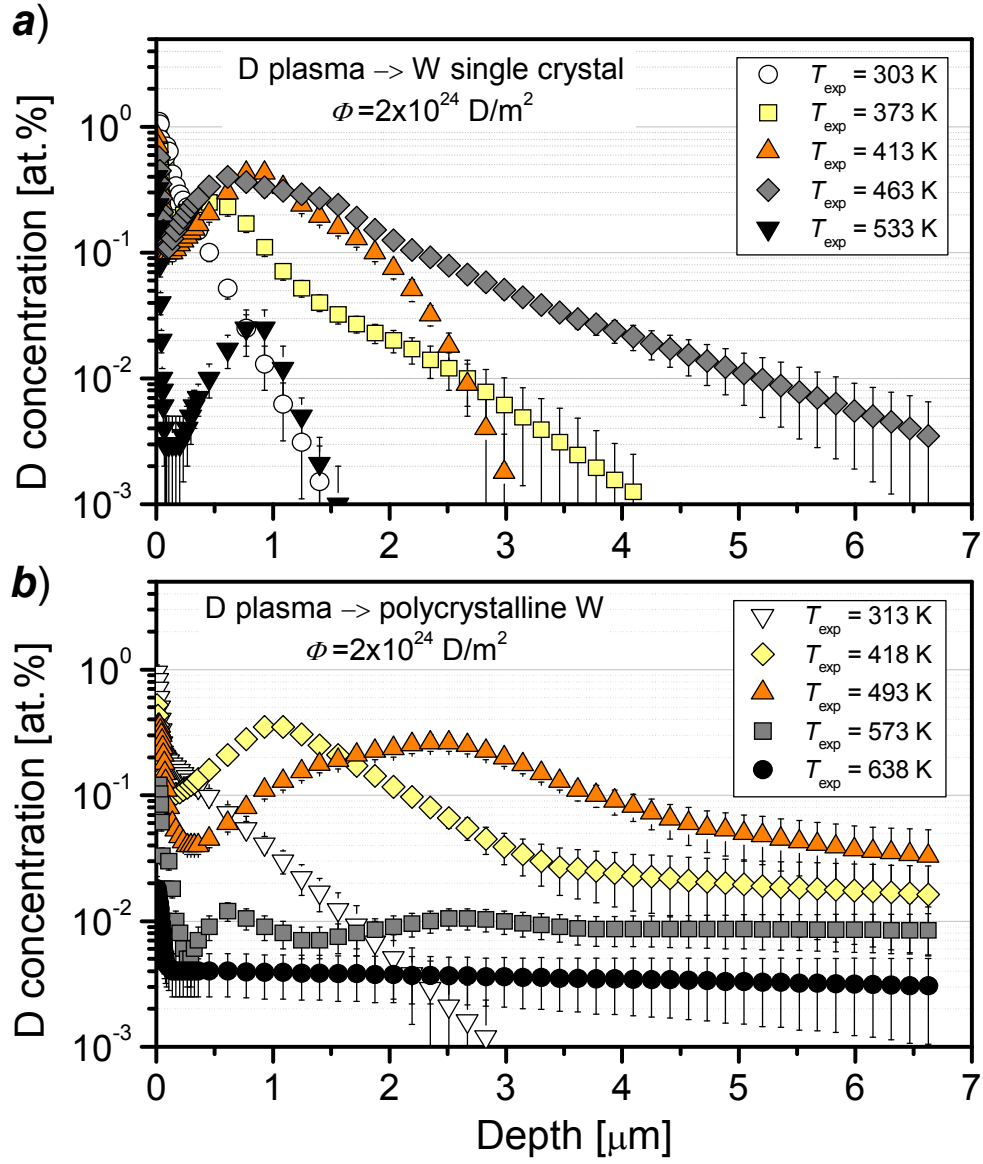[67] E.P. EerNisse, S.T. Picraux, J. Appl. Phys. 48 (1977) 9.

Fig. 1. Depth profiles of deuterium trapped in W single crystal (a) and polycrystalline W (b) exposed to a low-energy ($\approx$200 eV/D) and high ion flux (1.1×10^{21} m^{-2}s^{-1}) "clean" deuterium plasma to an ion fluence of 2×10^{24} D/m^2 at various temperatures.
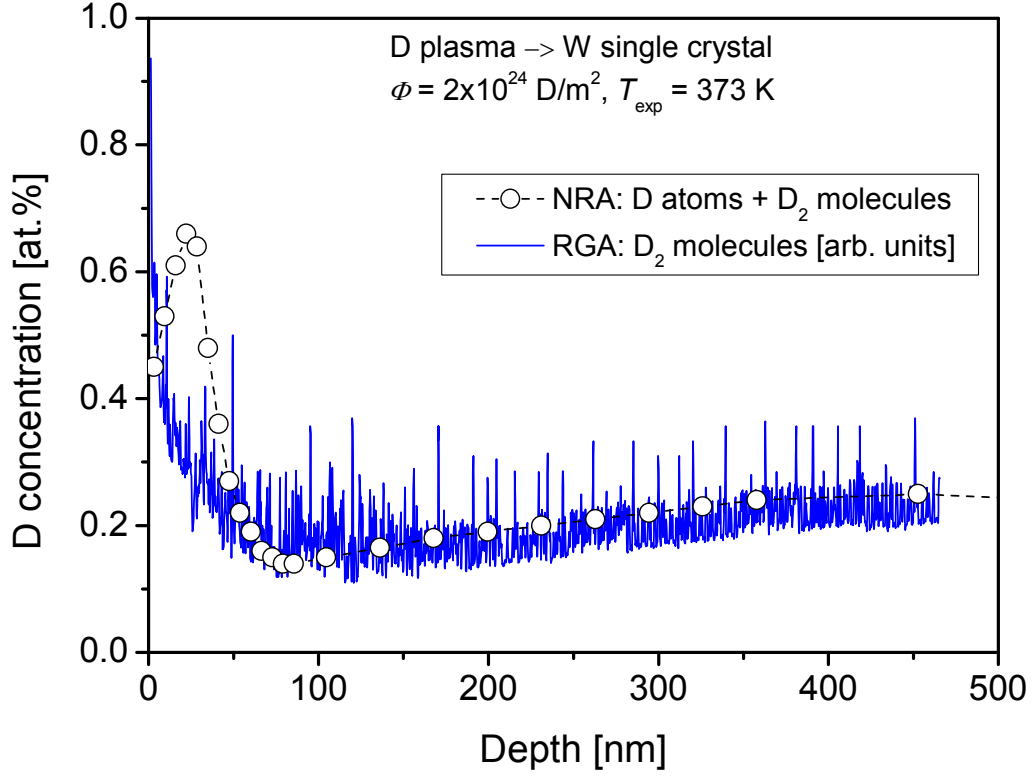
Fig. 2. Depth profile of deuterium in W single crystal exposed to a low-energy ($\approx$200 eV/D) and high ion flux (1.1×10^{21} m^{-2}s^{-1}) "clean" deuterium plasma to an ion fluence of 2×10^{24} D/m^2 at 373 K as measured with the D(^{3}He,α)H nuclear reaction (NRA) and with the sputter-residual gas analysis technique (RGA). Note that the concentration of D$_2$ molecules (RGA measurement) is given in arbitrary units.
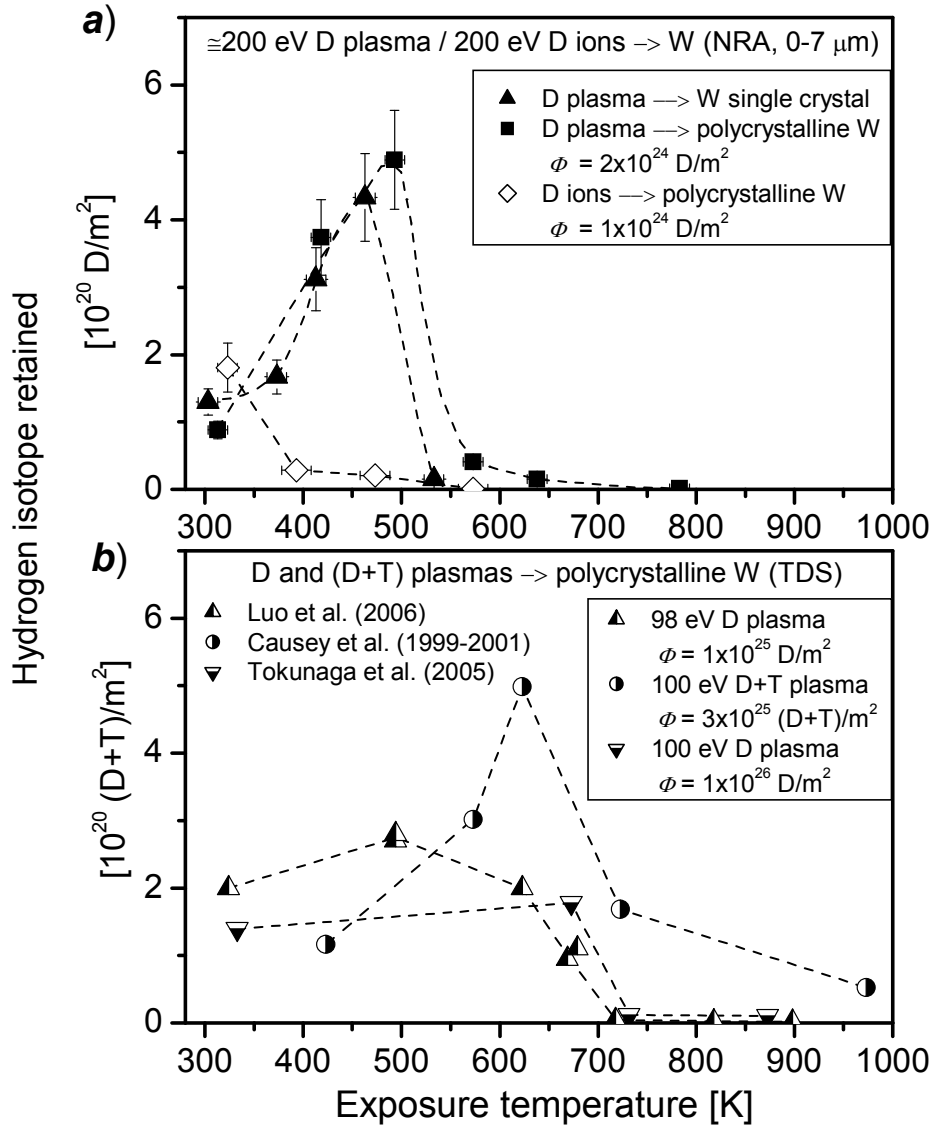
Fig. 3. a) Deuterium retention in single-crystalline and polycrystalline tungsten exposed to a low-energy ($\approx$200 eV/D) and high ion flux (1.1×10^{21} m^{-2}s^{-1}) "clean" deuterium plasma to an ion fluence of 2×10^{24} D/m^2 as a function of the exposure temperature. For comparison, the temperature dependence of the D retention in polycrystalline W irradiated with 200 eV D ions and flux of 4×10^{19} D/m^{2}s to a fluence of 1×10^{24} D/m^2 is also shown. The deuterium retention was calculated from deuterium depth profiles measured up to a depth of 7 μm.

b) Deuterium retention in polycrystalline tungsten exposed to low-energy (98-100 eV/D(T)) and high ion flux ($(0.9-1)\times10^{22}$ m^{-2}s^{-1}) "clean" D or (D+T) plasmas as a function of the exposure temperature [21, 27, 42, 45]. The D retention was examined by TDS.
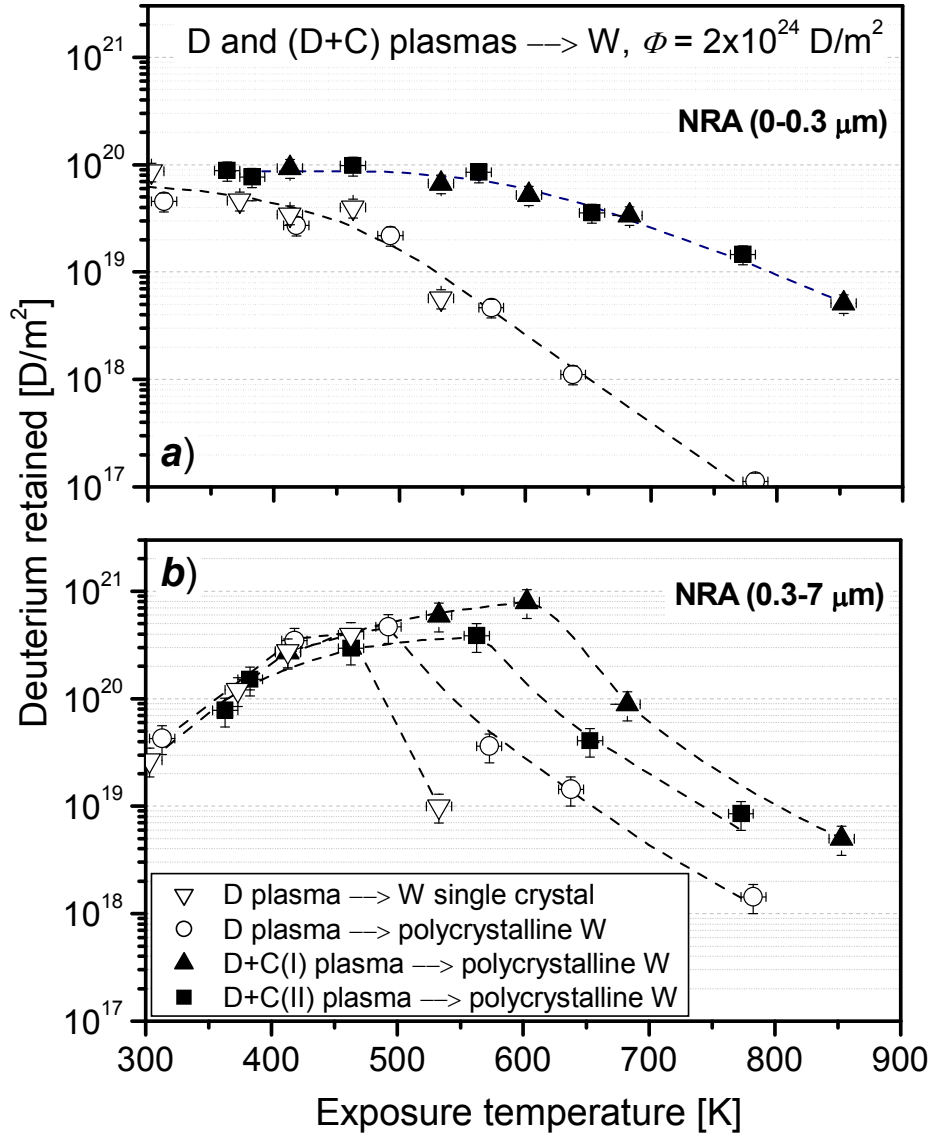
Fig. 4. Deuterium retention at depths of 0-0.3 μm (a) and at depths of 0.3-7 μm (b) in single-crystalline and polycrystalline tungsten exposed to a low-energy (≈200 eV/D) and high ion flux (1.1×10^{21} m^{-2}s^{-1}) "clean" and carbon-seeded deuterium plasmas to an ion fluence of 2×10^{24} D/m^2 as a function of the exposure temperature.
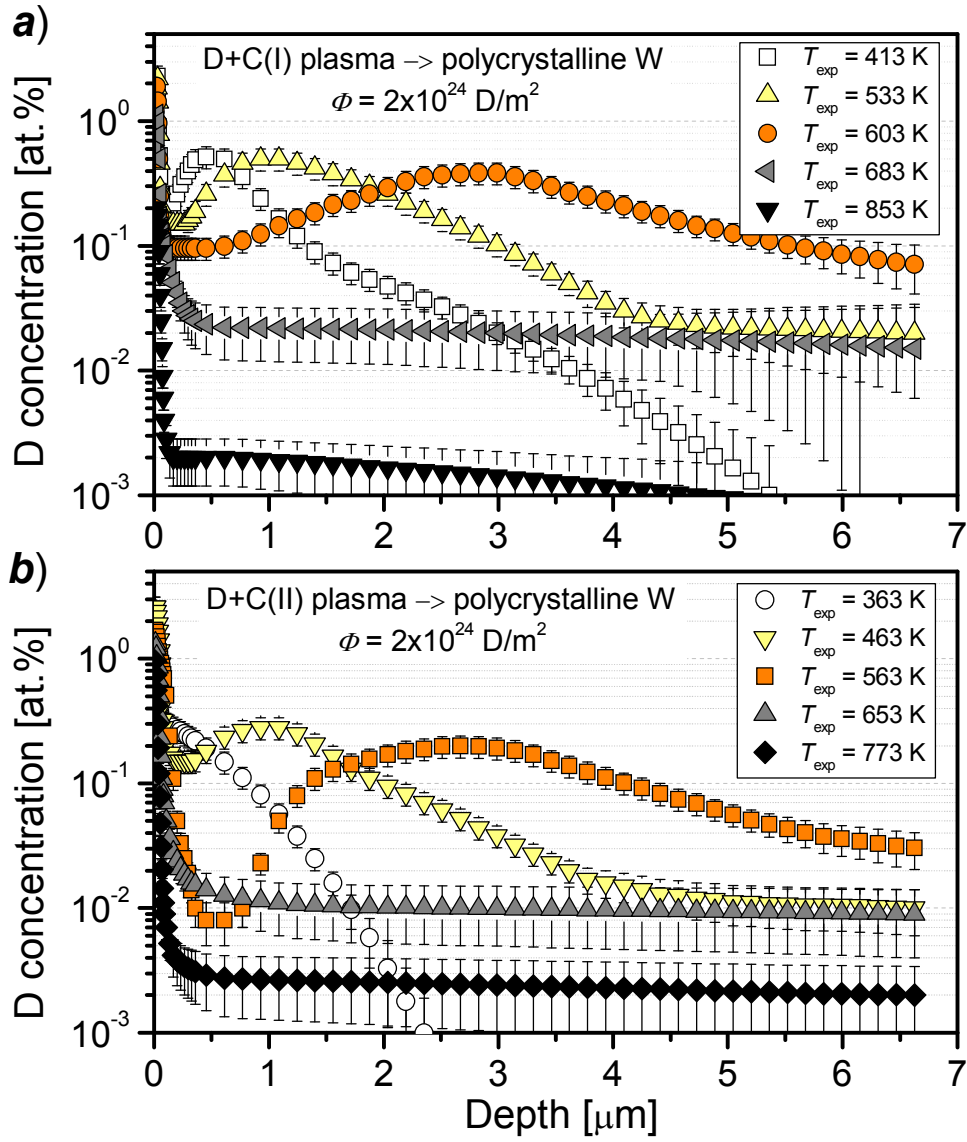
Fig. 5. Depth profiles of deuterium trapped in polycrystalline W exposed to a low-energy ($\approx$200 eV/D) and high ion flux (1.1×10^{21} m^{-2}s^{-1}) carbon-seeded deuterium plasmas to an ion fluence of 2×10^{24} D/m^2 at various temperatures.
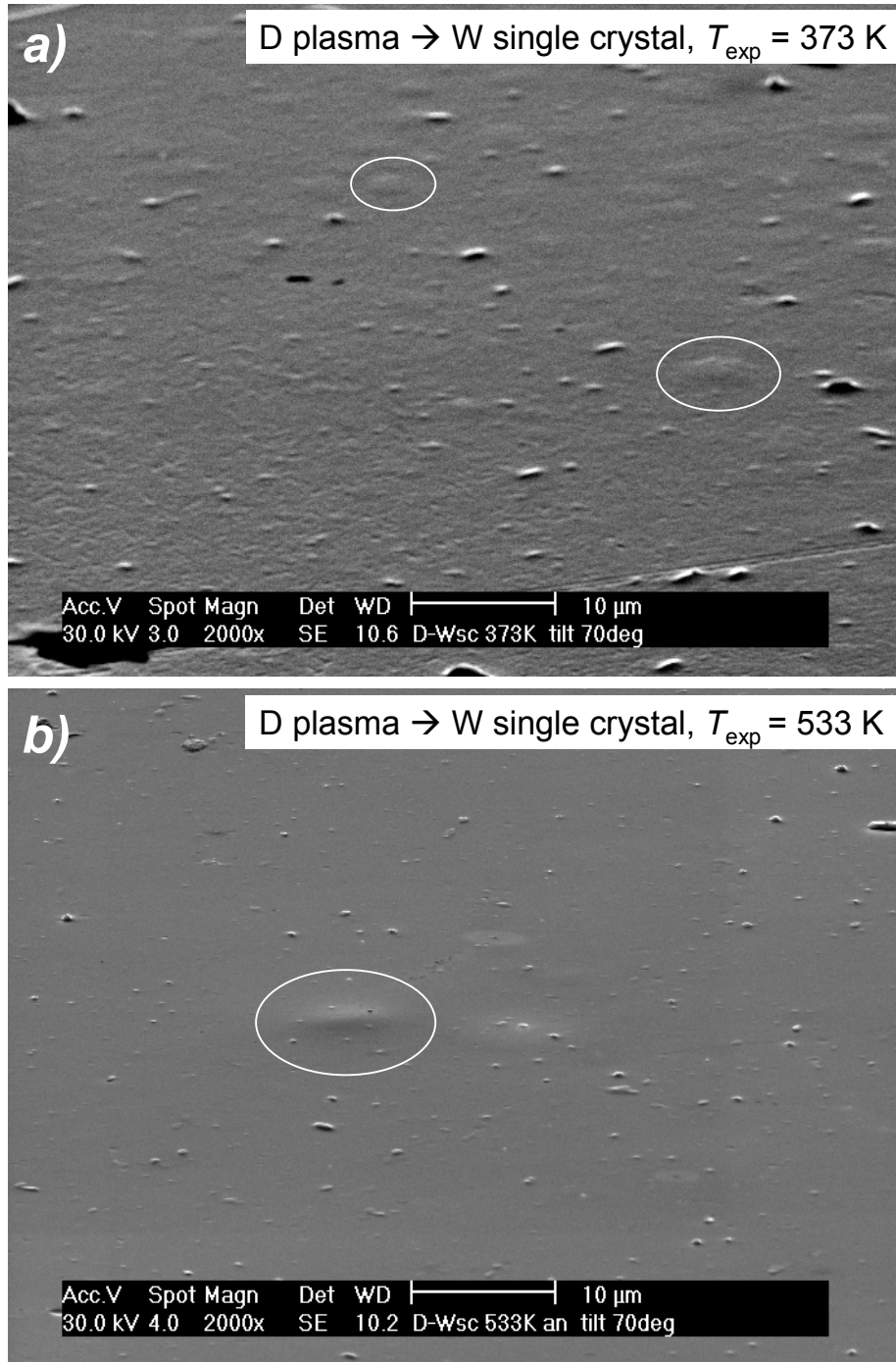
Fig. 6. Blisters formed on the surface of single-crystalline W exposed to a low-energy ($\approx$200 eV/D) and high ion flux (1.1×10^{21} $m^{-2}s^{-1}$) "clean" deuterium plasma to an ion fluence of 2×10^{24} D/m^2 at temperatures of 373 K (a) and 533 K (b). The surfaces were analyzed at a tilt angle of 70 degrees. Some of the blisters are marked by ovals.
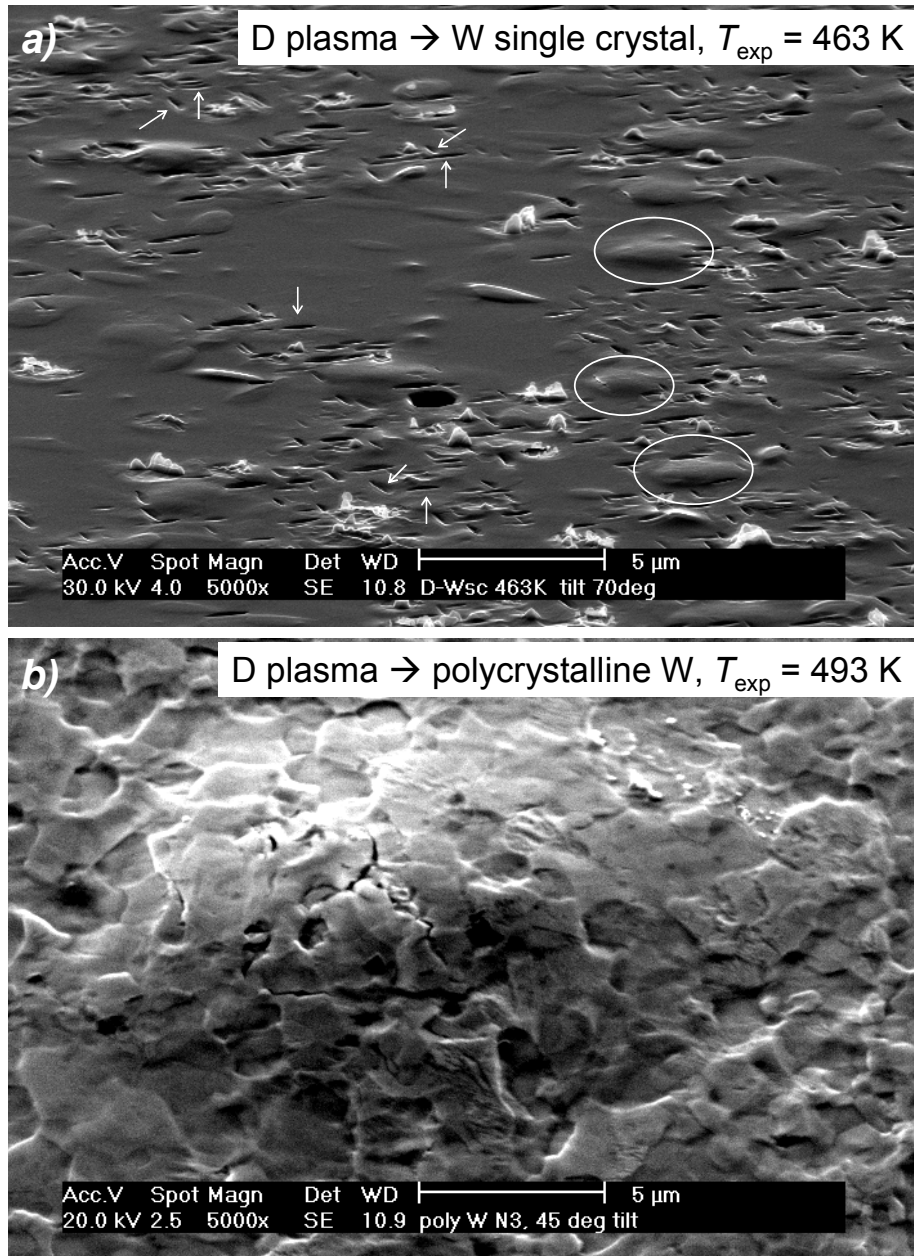
Fig. 7. SEM micrographs of W single crystal (a) and polycrystalline W (b) exposed to a low-energy ($\approx$200 eV/D) and high ion flux (1.1×10^{21} $m^{-2}s^{-1}$) "clean" D plasma to a fluence of about 2×10^{24} D/m^2 at 463 K (a) and 493 K (b). The surfaces were analyzed at tilt angles of 70 (a) and 45 (b) degrees. Some of the blisters on the surface of W single crystal (a) are marked by ovals, some of the etching pits are indicated by arrows.
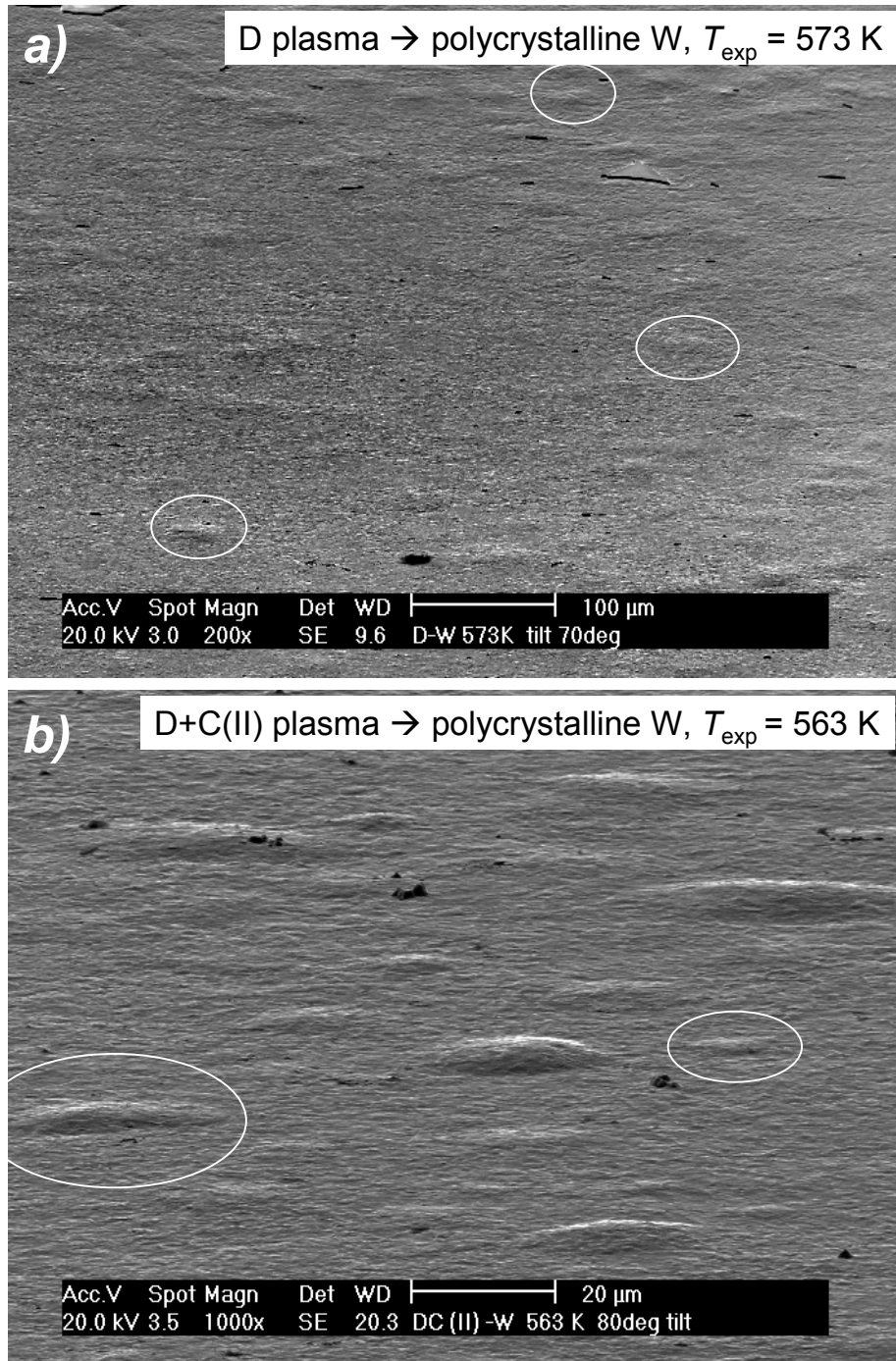
Fig. 8. Blisters formed on the surface of polycrystalline W exposed to a low-energy ($\approx$200 eV/D) and high ion flux (1.1×10^{21} m^{-2}s^{-1}) "clean" (a) and carbon seeded (b) D plasmas at T_{exp} = 563-573 K to an ion fluence of 2×10^{24} D/m^2. The surfaces were analyzed at tilt angles of 70 (a) and 80 (b) degrees. Some of the blisters are marked by ovals.
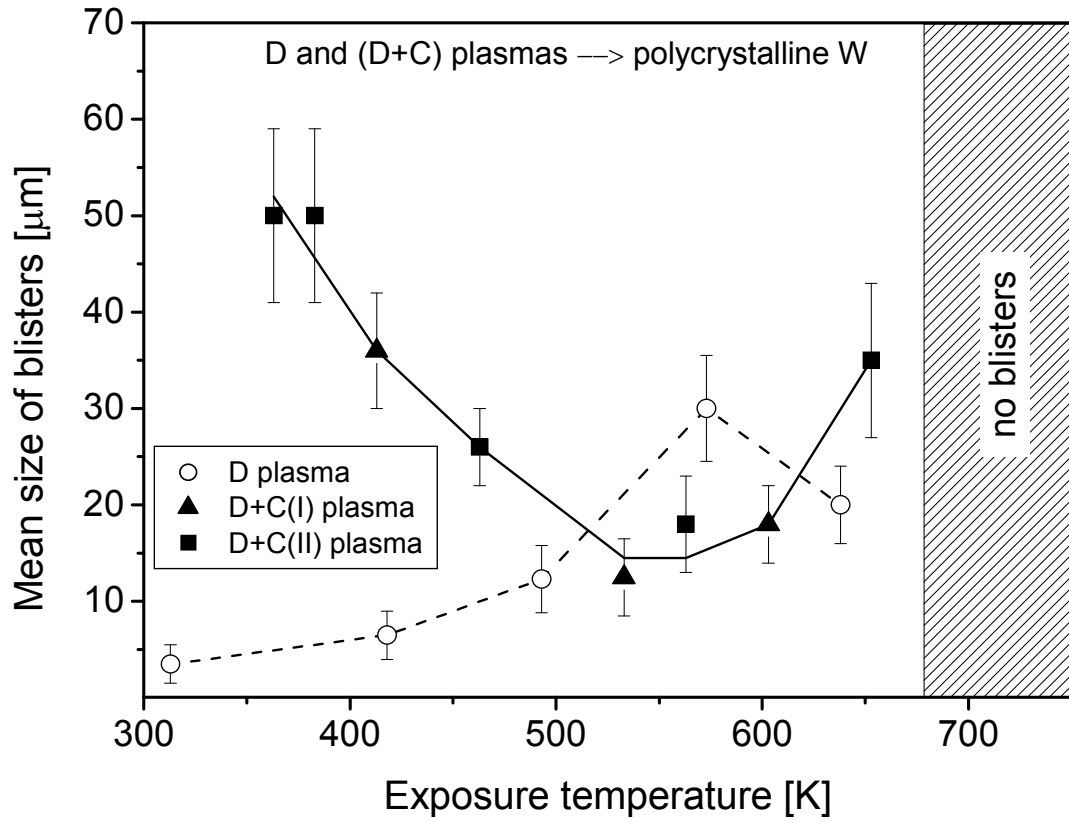
Fig. 9. Mean size (diameter) of blisters formed on the surface of polycrystalline W exposed to a low-energy ($\approx$200 eV/D) and high ion flux (1.1×10^{21} m^{-2}s^{-1}) "clean" and carbon-seeded D plasmas to an ion fluence of 2×10^{24} D/m^2, as a function of the exposure temperature.
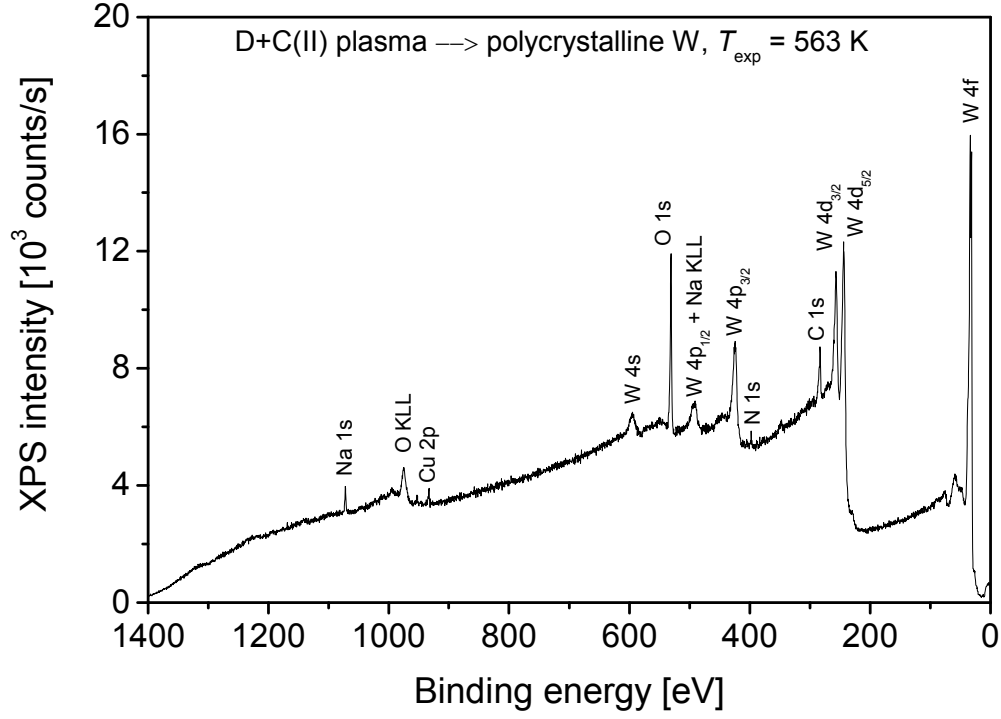
Fig 10. Survey XPS spectrum of polycrystalline W exposed to a low-energy ($\approx$200 eV/D) and high ion flux (1.1×10^{21} m^{-2}s^{-1}) "D+C(II)" plasma at T_{exp} = 563 K to an ion fluence of 2×10^{24} D/m^2. The XPS measurement was performed after surface sputtering with 3 keV Ar ions at a fluence of 1×10^{19} Ar/m^2.
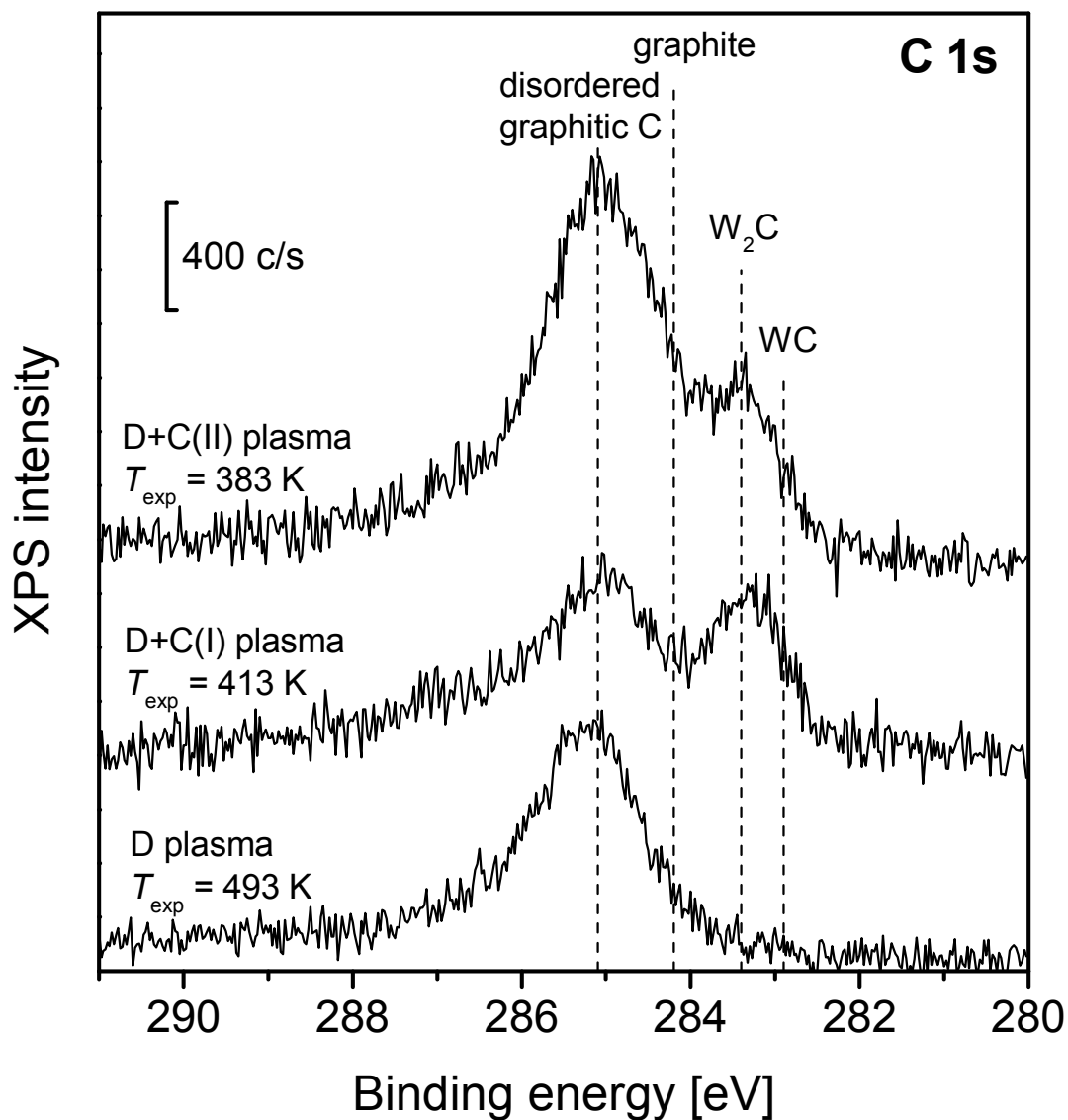
Fig. 11. C 1s core-level XPS spectra of polycrystalline tungsten exposed to a low-energy ($\approx$200 eV/D) and high ion flux (1.1×10^{21} $m^{-2}s^{-1}$) "clean" and carbon-seeded D plasmas to an ion fluence of 2×10^{24} D/m^2. The XPS measurements were performed after surface sputtering with 3 keV Ar ions at a fluence of 1×10^{19} Ar/m^2.